Investigative Ophthalmology and Visual Sciences

Effects of vitreous liquefaction on the intravitreal distribution of sodium fluorescein, fluorescein dextran and fluorescent microparticles

LE. Tan[1], W. Orilla[2], P.M. Hughes[2], S. Tsai[2], J.A. Burke[2], C.G. Wilson[1,3]

[1] Strathclyde Institute of Pharmacy and Biomedical Sciences, University of Strathclyde, 27 Taylor Street, Glasgow G4 0NR, UK.

[2] Allergan, Inc., 2525 Dupont Drive, Irvine, California 92612, USA.

[3] To whom correspondence should be addressed. (e-mail: c.g.wilson@strath.ac.uk)

Word Count: 3761

Commercial Relationships: L.E. Tan, F; **W. Orilla**, E; **P.M. Hughes,** E; **S. Tsai**, E; **J.A. Burke,** E; **C.G. Wilson,** C.

Financial Support: LET is the recipient of an open educational scholarship from Allergan Inc.

Declaration statement: Part of the data has been presented at ARVO 2009 Summer Eye Research Conference, NIH Bethesda, Maryland.

Abstract:

Purpose: The effects of vitreous liquefaction in the elderly on the distribution of drugs from intravitreal injections, depots or devices remains unclear. The aim of the present study was to develop a liquefied vitreous model that simulates the aged condition, allowing the study of clinically relevant drug distribution.

Methods: Dutch-belted rabbits were used to develop a study model using hyaluronidase as a vitreolytic agent. The effects of experimental vitreous liquefaction were investigated on intravitreal sodium fluorescein, fluorescein isothiocyanate-dextran (MW= 150kDa) and a suspension of 1 μm fluorescent particles. The distribution of these model compounds was monitored using Heidelberg Retinal Angiography (HRA) confocal laser scanning system and ocular fluorophotometer.

Results: Hyaluronidase-treated vitreous humor (n=6) was found to decrease the gel phase to 41 ± 9% (w/w; mean ± SD) as compared to 81 ± 9% in the control eyes (n=8) ($p<0.05$). The distribution of sodium fluorescein and fluorescein isothiocyanate dextran was greater in the liquefied vitreous than control. In comparison to the normal vitreous, fluorescent particles sedimented faster in the liquefied vitreous and the distribution was more dispersed and scattered.

Conclusions: A model of vitreous liquefaction in rabbits was successfully generated using intravitreal hyaluronidase. Small and large fluorescent molecules as well as particulates distributed faster in liquefied vitreous as

compared to control. This suggests enhanced convective flow, and subsequent faster clearance in liquefied vitreous.

Introduction

The volume of the human vitreous humor is approximately 4mL, and forms the largest (80%) compartment of the globe in the posterior segment of the eye[1]. This makes the vitreous a readily available drug reservoir for the treatment of retinal diseases. The main composition of the vitreous is water (>98%) but its three dimensional microstructure is primarily constituted by the remaining 1% of structural elements, mainly collagen and proteoglycans[2]. In a juvenile vitreous humor approximately 80% of the water is bound, trapped within the collagen-hyaluronan gel network; while the remainder (~20%) is in the form of free water constituting the liquid phase[3].

With aging, the vitreous degenerates progressively and collagen fibrils, which are kept apart by proteoglycans in the juvenile eye aggregate into coarse fibers[4-6]. The detached collagenous fragments, together with cells and pigment, are clinically perceived as 'floaters' by most patients. In addition, the hyaluronan component segregates into a pool of free water, presumably as a result of depolymerization of its linear chain[1]. The vitreous of an elderly patient (>60 years old) will therefore have a higher content of free water with a gel-liquid ratio of approximately 1[3]. Most of the populations treated for many posterior segment diseases such as age-related macular degeneration are by definition elderly. Previous literature contributed by vitreo-retinal surgeons have described the role of vitreous structure as a diffusional barrier[7,8] and have considered the implications of loss of vitreous gel structure to movements of material around the eye[9-13].

However, the preclinical design of treatment regimens for most ocular problems are largely based on young animal models, rabbits and rats, having a fully formed vitreous with a high gel content (~80%). For this reason, the impact of vitreous liquefaction on the distribution of drugs and carriers has largely been ignored. This led to the aim of the current study, which was to quantitatively and reproducibly generate a partially (~50%) liquefied vitreous model in laboratory rabbits that mimics the aged condition to better assess drug disposition in the aged eye.

Materials and Methods:

Preparation of hyaluronidase, sodium fluorescein, fluorescein isothiocyanate-dextran (FD) 150kDa solutions and 1μm fluorescent particle suspension

Lyophilized ovine testicular hyaluronidase with enzyme activity of ≥ 1000 I.U./mg (MP biomedical, OH, USA) was reconstituted with 0.9% normal saline and serial dilution was performed to produce hyaluronidase injection solutions of concentration 0.005I.U./20μL. Fluorescein isothiocyanate-dextran, average molecular weight 150kDa (Sigma, St. Louis, MO), was dissolved in 0.9% normal saline to produce a 0.01 %(w/v) solution. A 10 %(w/v) sodium fluorescein solution (Akorn, Inc., Buffalo Grove, IL) was diluted in 0.9% normal saline to 0.01 %(w/v) prior to use. A 1μm fluorescent polystyrene latex microsphere suspension (Fluoresbrite®) was purchased from Polysciences Inc. PA and was used without further dilution.

In vivo model of vitreous liquefaction

All animal handling procedures involved in this study were approved by the Allergan Animal Care and Use Committee and complied with the ARVO statement for the use of animals in ophthalmic and vision research. Fourteen Dutch-belted rabbits weighing 2-3kgs of ages ranging from 3 months to 2 years old were involved in the development phase of the model. Before the start of all experiments, the eyes of all animals were examined externally to exclude abnormalities. Prior to intravitreal injections, the rabbits were locally anaesthetized using topical 0.5% Tetracaine HCl ophthalmic solution USP (Bausch and Lomb, Tampa, FL) and their pupils were dilated using topical 10% Phenylephrine HCl (Akorn, Inc., Buffalo Grove, IL) and 1% Tropicamide USP (Alcon Laboratories, Fort Worth, TX). Twenty µL of hyaluronidase solutions of 0.005 I.U. (n=11) were intravitreally injected to induce vitreous liquefaction; while another 4 animals received bilateral injections of 20 µL normal saline to act as control. The animals were euthanized 24 (n=5) or 48 hours (n=6) later with intravenous injection of pentobarbital (Eutha-6, Western Medical Supply Co., Arcadia, CA), and the eyes were enucleated and dissected to obtain the vitreous humor. The vitreous samples were then collected onto a petri dish and the gel-liquid ratio was determined by first weighing the entire vitreous then weighing the liquid phase after removing the gel phase with a pair of forceps. The percentage vitreous gel content was calculated as [(mass of gel phase/total mass of vitreous)*100%]. The significance of differences in the percentage gel phase between normal and enzyme-treated eyes was evaluated using the student t-test with the

significant level defined at p-value < 0.05. During the study, evidence for ocular toxicity was monitored using a fundus camera.

In vivo measurements of fluorophores distribution using Heidelberg Retinal Angiography (HRA) confocal laser scanning system and ocular fluorophotometer

After developing the model, nine animals were used to study the effects of vitreous liquefaction on material distribution. Twenty µL of 0.005 I.U. hyaluronidase solution was injected unilaterally to the animals leaving the contralateral eyes untreated (normal vitreous) to act as control. Forty eight hours later, animals received bilateral intravitreal injections of 10 µL 0.01% sodium fluorescein (n=3), 1% fluorescein isothiocyanate-dextran (FD) (MW= 150kDa) (n=3) or a suspension of 1µm fluorescent particles (n=3). The distribution of the injected fluorescent molecules was monitored for a month using the HRA 2 (Heidelberg Engineering, Vista, CA) with a wide-angle ocular Staurenghi 230 Scanning Laser Ophthalmoscope (SLO) retinal lens, and an ocular fluorophotometer (Ocumetrics. Inc., San Francisco, CA). HRA allows the imaging of fluorescent probes in both x- and y- axis while ocular fluorophotometer detects the fluorescent intensity along the optical (z) axis. Ocular fluorophotometer data of the study groups were compared using the student t-test with a confidence level of $p<0.05$ considered as statistically significance.

Image analysis

The experimental images obtained using HRA were analysed using an image processing feature in Matlab (The Mathworks Inc, Natick, MA) to quantitatively compare the retention of fluorescent mass of sodium fluorescein and FD 150kDa in the enzyme-treated and contralateral normal vitreous. Using this method, the degree of distribution and clearance of injected molecules was correlated to its fluorescent intensity (in pixels) detected within the vitreous chamber with lower intensities indicating faster rate of transport. By calculating the fluorescent intensity ratio of normal to liquefied vitreous, the relative distribution and clearance of both models can be compared.

Results

Development of a model of vitreous liquefaction

Figure 1 shows the degree of vitreous liquefaction induced by 0.005 I.U. of hyaluronidase with either 24 hours or 48 hours post-dosing period. The 24 hours post-injection period produced a lower degree of liquefaction (77.9 ± 6.1%; $p>0.05$) as compared to that of 48 hours post-injection period.

In addition, 0.005 I.U. dose with post-injection period of 48 hours generated the target degree of vitreous liquefaction in rabbits in a reproducible fashion. In comparison to control, there was slight haziness in the vitreous chamber of hyaluronidase-treated eye but no gross ocular tissue changes identified (Figure 2). This model was then used to assess the effects of vitreous liquefaction on the disposition of three model compounds injected intravitreally.

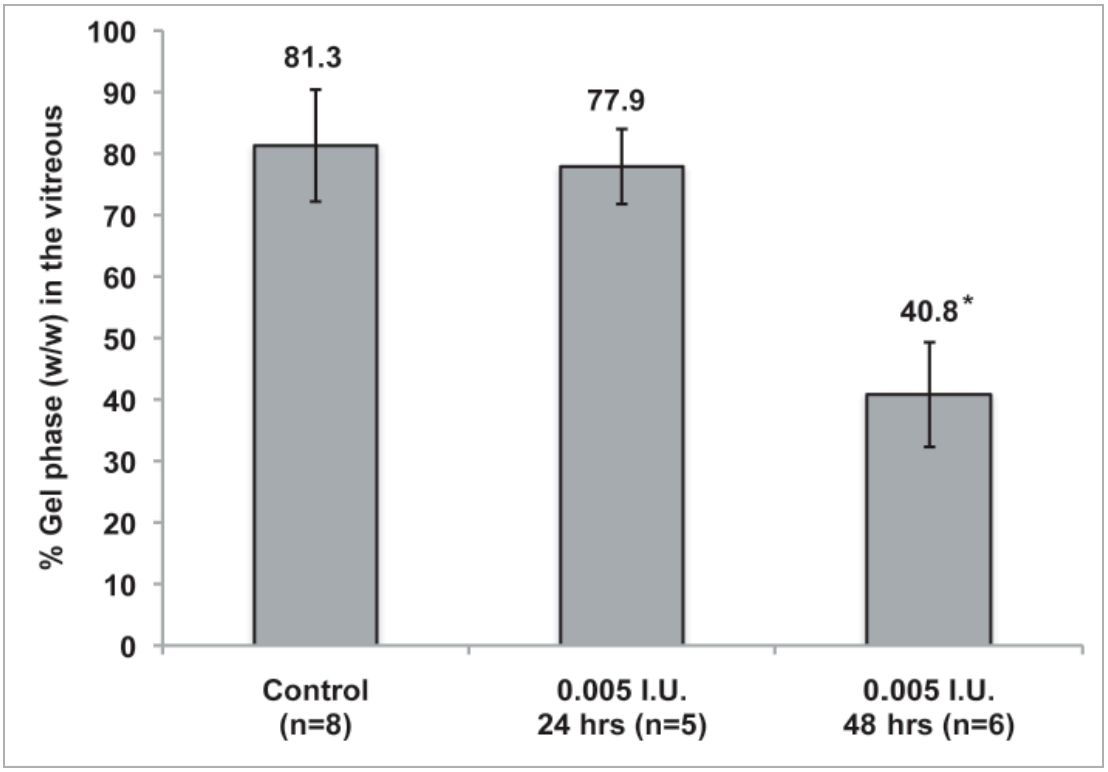

Figure 1: Percentage vitreous gel phase of control and hyaluronidase-treated groups. The difference in percentage gel phase between control and 0.005 I.U. (48 hours post-injection) hyaluronidase-treated group was statistically significant * ($p < 0.05$).

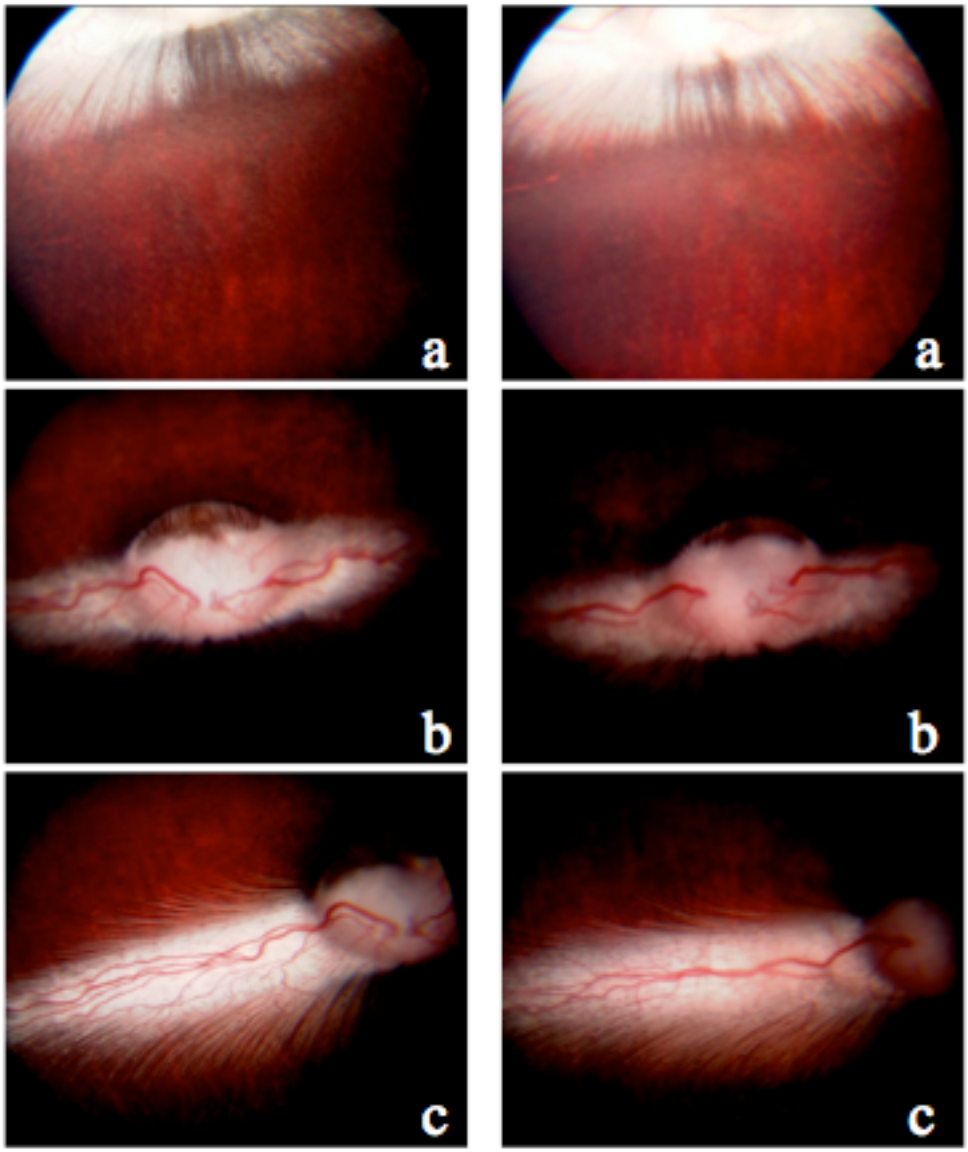

Figure 2: Fundus assessments of the medullary rays and optic nerve head in control (left panel) and hyaluronidase-treated (right panel) eyes. a: Medullary rays; b: Optic nerve head; c: Right medullary rays and optic nerve head.

Effects of vitreous liquefaction on the dispersion of model compounds

I. Sodium Fluorescein

Figure 3 shows a set of representative HRA images comparing the intravitreal distribution of sodium fluorescein in both normal (control) and liquefied (hyaluronidase-treated) vitreous at 2 and 5 hours after injection. The fluorescent depot in the liquefied vitreous spread out faster from the injection

pocket and perhaps from the vitreous cavity. An analysis constructed using the Matlab programme used in our laboratories indicated that sodium fluorescein clearance as measured by fluorescence intensity was 1.4 and 1.5 times faster in the liquefied vitreous at 2 hours and 5 hours respectively as compared to that measured in control. Figure 4 shows the distribution profiles along the z-axis of the eye at 2 hours and 5 hours for both models. At the same injected dose, sodium fluorescein concentration was found to be lower in the liquefied vitreous at all times ($p<0.05$). However, the fluorescent mass distributed with a similar concentration gradient in both models. The plateau in the control eye data at 2 hours between 17 and 21 mm from the origin probably indicates penetration into the lens. The probe does not continue a forward diffusion since the vectoral fluid flow in the lens opposes diffusion, unloading absorbed fluorescein back into the vitreous humour at 5 hours post administration[14]. The behaviour is less obvious in the liquefied vitreous, presumably because the concentration gradient cannot be sustained. Table 1 is a summary of the HRA and ocular fluorophotometry results for the study models.

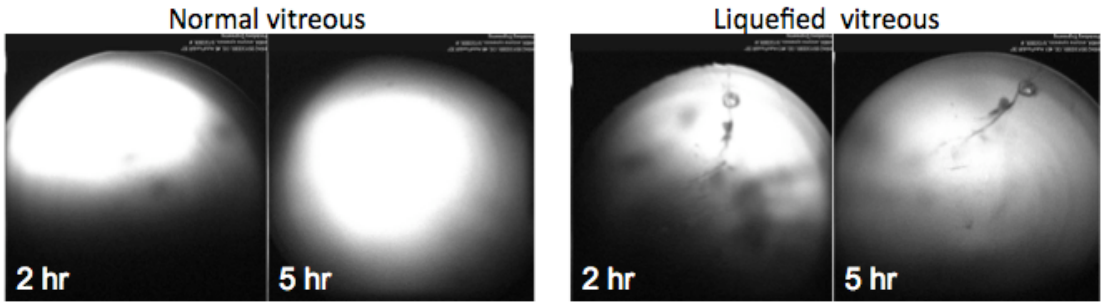

Figure 3: Representative HRA images obtained from one animal 2 hours and 5 hours after receiving 10μL intravitreal injection of sodium fluorescein solution. The fluorescent mass was well retained in the intact vitreous after 5 hours but is more diffuse in liquefied vitreous.

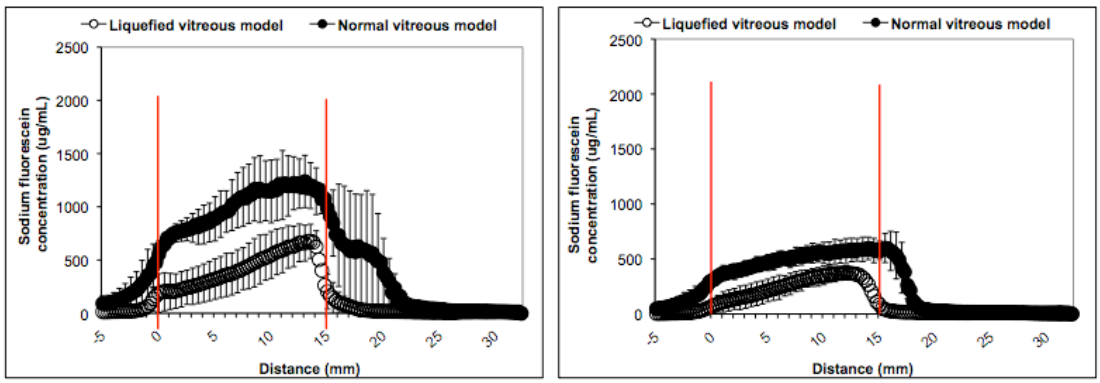

2 hours 5 hours

Figure 4: Ocular fluorophotometry of intravitreally injected sodium fluorescein depot at 2 hours (left) and 5 hours (right) after injection (n=3). On these graphs, zero mm represents the vitreo-retinal interface while 15 mm represents the back of the lens.

II. Fluorescein dextran (FD) 150kDa

Figure 5 is a set of representative HRA wide-angle images obtained from one animal comparing the distribution of FD 150kDa in the vitreous cavity over a period of one month. The figure also shows that the FD 150kDa solution formed a defined depot that lasted for at least 5 hours after injection and gradually spread across the vitreous chamber thereafter as indicated by the increasing diameter of the fluorescent mass. There was no significant difference in the distribution of FD 150kDa between the models until day 3. However, from day 6 onwards, the amount of FD 150kDa, which remained in the vitreous was lower in the liquefied model as compared to control. There was no residual FD 150kDa detected optically in the liquefied vitreous model on day 30 but a low degree of fluorescent intensity remained visible in the normal vitreous, suggesting FD 150kDa had a shorter intravitreal half-life in the liquefied vitreous. Figure 6 shows the graph generated using Matlab to calculate the fluorescent intensity of FD 150kDa remaining in the vitreous

humor over time. The y-axis on the plot represents fluorescent intensity (in pixels) remaining within the vitreous cavity and the scale is in arbitrary units. FD 150kDa was cleared faster in the liquefied vitreous as compared to the normal vitreous model. Figure 7 shows the plots obtained from the ocular fluorophotometry study. At one hour after injection, most of the injected FD 150kDa remained at the site of injection in both models. However, the 2 and 5 hours data suggest that FD 150kDa moved towards the anterior chamber in the liquefied vitreous, while remaining in place in the normal vitreous. On day 2, FD 150kDa started to spread across the optical axis as shown by the more even fluorescence distribution. Additionally, the fluorescence gradient was steeper in the liquefied vitreous than the normal vitreous on days 2 and 3. On day 6 the gradient decreased, indicating that the initial phase of diffusive equilibration was completed. This data was in agreement with the HRA wide-angle image, where the fluorescent intensity was evenly distributed across the chamber for the liquefied vitreous. In the normal vitreous, the general fluorescence gradient did not change considerably over similar time periods. As the FD 150kDa was cleared from the vitreous cavity of the study models, the fluorescent intensity reduced in both x- and y-axis as detected by HRA and ocular fluorophotometry. Statistical analyses showed that the fluorescent intensity of FD 150kDa was significantly higher ($p<0.05$) in normal vitreous on day 21 and day 30, which agreed with HRA observations.

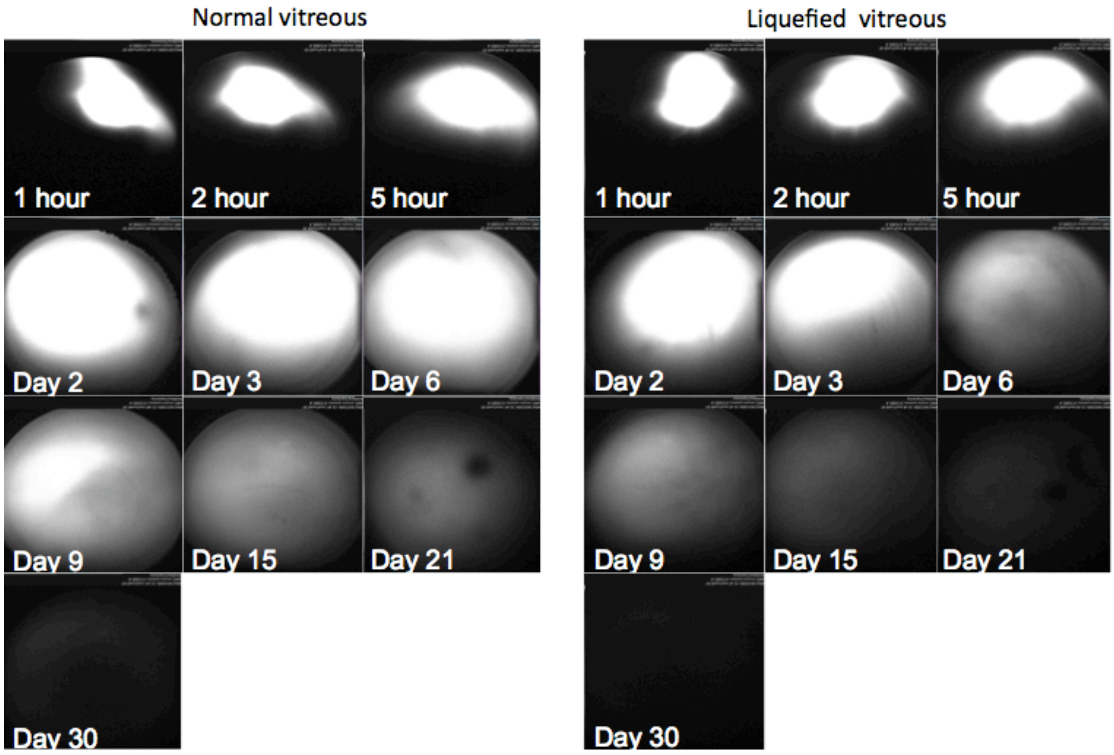

Figure 5: HRA wide-angle images of intravitreally injected fluorescein dextran 150kDa in the normal and liquefied vitreous models from 1 hour to day 30 after injection.

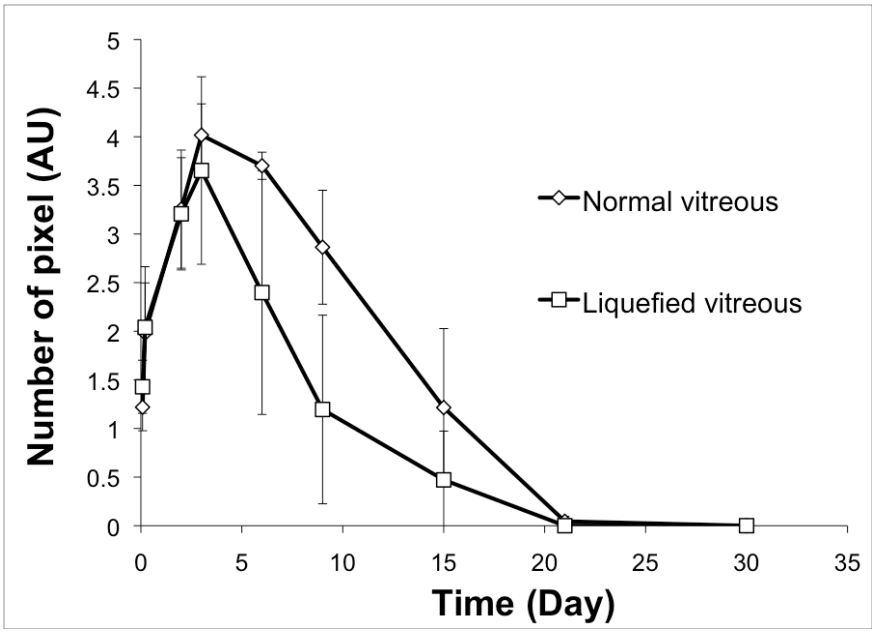

Figure 6: Plot generated using Matlab (based on HRA images) comparing the fluorescent intensity of FD 150kDa from 2 hours to 30 days after injection in both liquefied and normal vitreous models. Means (n=3) ± standard deviations are shown. The curves were consistent with the HRA findings.

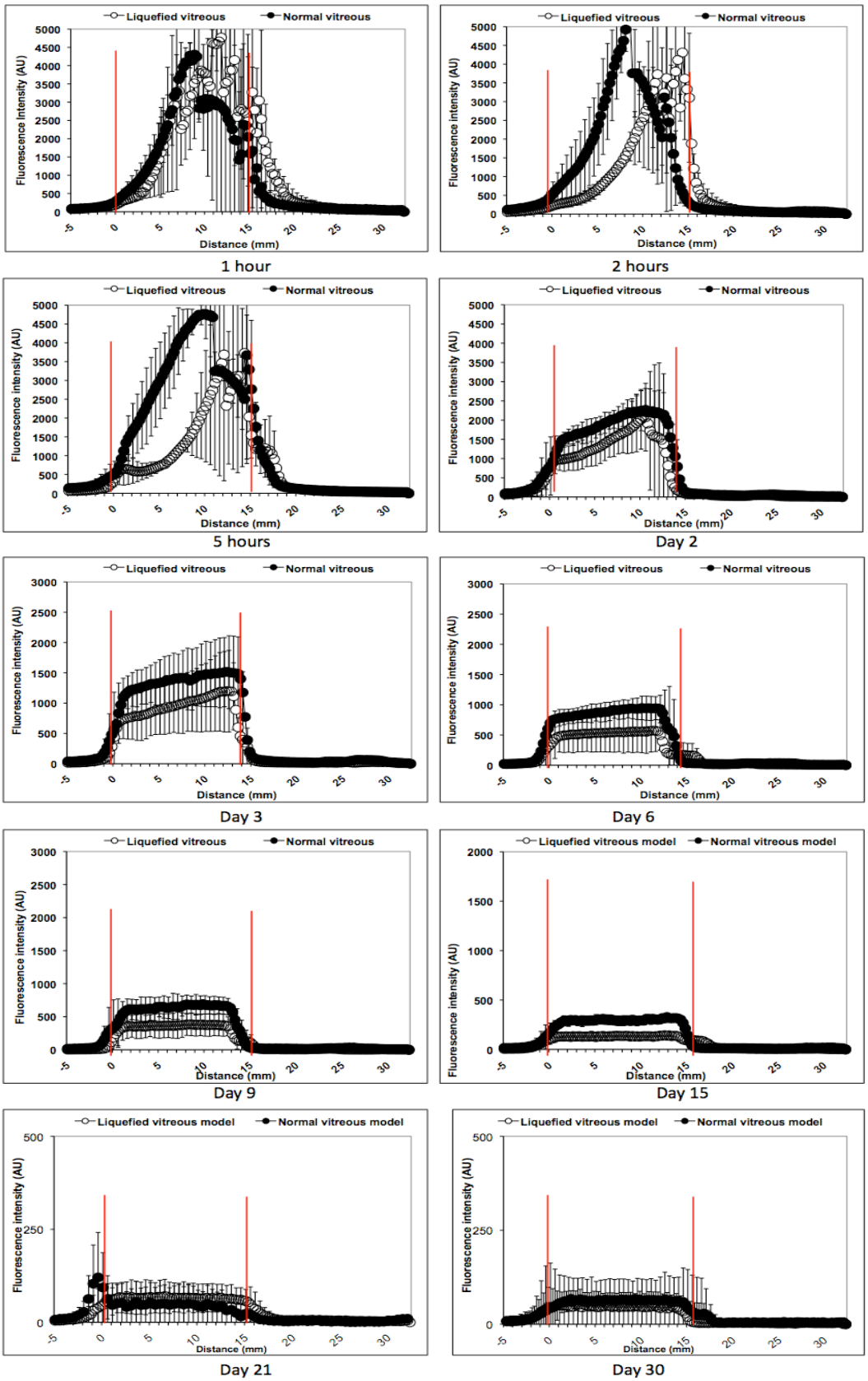

Figure 7: Ocular fluorophotometry data obtained from the study animals showing the fluorescent intensity along the optical axis from the back of the lens (15mm) through to surface of the retina (0mm).

	Sodium Fluorescein			Fluorescein Dextran (FD) 150kDa									
Time points	1 hr	2 hr	5 hr	1 hr	2 hr	5 hr	D2	D3	D6	D9	D15	D21	D30
HRA Intensity ratio	1.1	1.4	1.5	0.87	0.84	0.97	1.04	1.15	2.6	3.8	>10	>10	2.17
OF Student t-test	p<0.05 *			p>0.05	p<0.05 *								

Table 1: The summary data for sodium fluorescein and FD 150kDa in the study models. HRA results were presented as the fluorescent intensity ratio of normal to liquefied vitreous. While the average sodium fluorescein concentration and average fluorescent intensity of FD150kDa obtained from ocular fluorophotometry (OF) analysis were compared using student t-test. Hr: hour; D: day.

*: Average concentration of sodium fluorescein and fluorescent intensity of FD 150kDa were significantly lower in partially liquefied vitreous at all time points except at 1 hour after injection of FD 150kDa.

III. 1μm particle suspension

The intravitreal distribution of 1μm fluorescent particles was assessed using HRA. The images obtained are shown in Figure 8. Gravitational forces resulted in sedimentation of microparticles in the liquefied vitreous model on day 9 whilst microparticles in the normal vitreous settled later. In the normal vitreous, microparticles sedimented without much lateral diffusion as opposed to the liquefied vitreous where the particles appeared more dispersed and scattered.

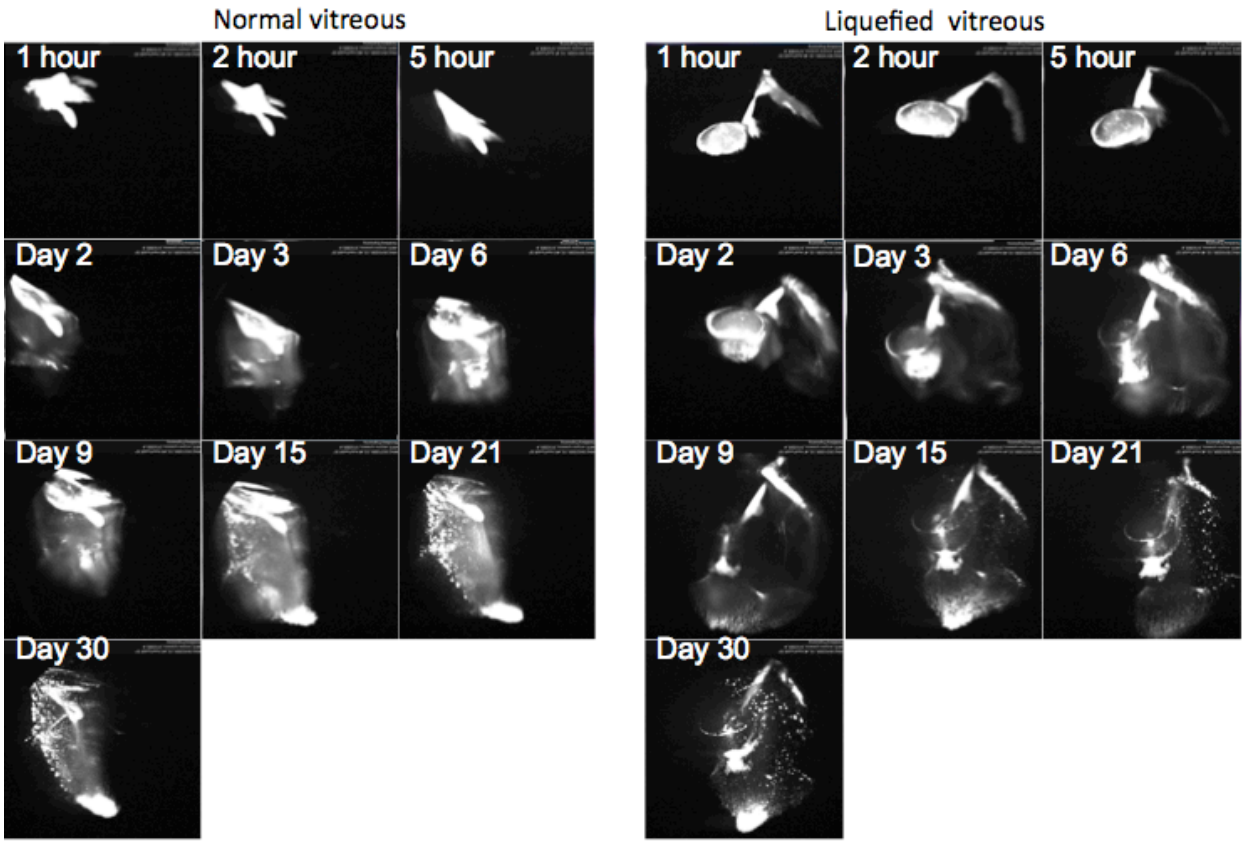

Figure 8: A representative set of HRA images obtained from one of the three animals involved in this study. The images were taken from 1 hour until day 30 after injection. The upper part of the image represents the superior area of the rabbit vitreous. Microparticles remained relatively in place at the injection site (superior-temporal) in both models for at least 5 hours post-injection.

Discussion

In this study, a partially liquefied vitreous model was successfully developed in Dutch-belted rabbits for ocular drug delivery research. To the best of our knowledge, no study to date has quantitatively established a partially liquefied vitreous model using hyaluronidase. Several studies have described intervention for vitreo-retinal problems employing hyaluronidase to induce posterior vitreous detachment (PVD) with varying success[15-17]. Tanaka[18], Gottlieb[19] and others[20,21] have demonstrated that vitreous liquefaction was feasible following hyaluronidase injection without quantifying the degree of liquefaction.

In addition, our data shows that in an unmodified rabbit vitreous only ~20% of its content was composed of a liquid phase, which was similar to that of young human adults[3]. Hyaluronidase liquefied the vitreous by cleaving the glycosidic bonds of the vitreous hyaluronan and changed its structural conformation[22]. The resultant depolymerization altered its hydration property leading to the release of bound water as indicated by the increase in vitreous liquid volume and decrease in the gel wet weight observed in this study. We concluded that 0.005I.U./20uL with 48 hours exposure time period achieved the target degree of liquefaction representative of the elderly vitreous. Bracketing this concentration with single point administrations at higher and lower amounts of enzyme suggested that this concentration and exposure time is optimal. In further studies with this model in-house, we have seen no further changes in the sol-gel ration between 3 and 30 days post-injection of the enzyme, administered to similar animals at the same doses. This observation was further supported by the literature, which has reported that hyaluronidase-induced disaggregation of vitreous hyaluronic acid remained for at least a month before being replaced by the newly formed hyaluronic acid[21]. Based on the old observations by Pirie, it was possible that partial vitreous liquefaction persisted for the entire duration of experiment. Nevertheless, we were unable to confirm in this study if the liquefaction generated was in the form of bulk fluid or several liquid pockets embedded in the gel phase. This process will have to be further investigated.

The inter-animal variability (~9%) was similar in both normal and hyaluronidase-treated groups, emphasizing the robustness of the liquefied model. In addition, it has been reported that hyaluronidase was non-toxic to

rabbit retina at a dose of 1U[19]. The safety of this enzyme was not a prime objective investigated in this study but no gross ocular tissue changes were observed with fundus examination.

Three model compounds were selected to assess the impact of partial vitreous liquefaction on the intravitreal movements of molecules with different molecular weights. The molecular size of sodium fluorescein can be a representative compound to many intravitreal antimicrobial agents and steroids used in the treatments of ocular infection and inflammation. FD 150kDa is a large molecule and thus the molecular size might model for antibodies such as bevacizumab. While 1 μm fluorescent particles can be representative of the sizes used in microparticulate delivery systems, they are also ideal for examining intravitreal convective flow since diffusive movement is limited for this object size. Drug movements within the vitreous chamber and their intravitreal life-time depend largely on molecular size. Our data shows that FD 150kDa spread slower and had a longer intravitreal half-life of approximately 30 days as compared to sodium fluorescein, which was cleared within 48 hours. Microparticles, which were the largest among others, remained in the vitreous for longer than a month. These common findings with respect to larger molecules being retained better in the vitreous as compared to smaller molecules have been documented[23]. The likely explanation for this phenomenon is that the diffusion process of larger molecules is limited by the barrier functions of collagen-hyaluronan network[24]. Unlike small molecules, which can diffuse in all directions, macromolecules have to move in between the porous gel meshwork and thus, the transport process is largely depending on convective flow[23,25,26].

Ocular fluorophotometry shows the presence of concentration gradient across the vitreous chamber with the highest concentration near the anterior chamber and the lowest at the vitreo-retinal surface, suggesting diffusion was leading towards the retina. The clearance pathways of sodium fluorescein and FD 150kDa were not investigated in this study. However, Araie[27], Maurice[27,28] and Cunha-Vaz[28] based on their work in examining the vitreous sections of the frozen eye following intravitreal injection of fluorescent molecules have related this type of distribution pattern to retinal clearance. Fluorescein is a small hydrophile and its clearance from the vitreous appears to be aided by a small nucleotide transporter, termed P2Y2[29]. However, FD 150kDa is a relatively large molecule, hydrophilic in nature, which is not transported by this route, and permeation through the retinal layer remained in question. Dias and Mitra[30] attributed this observation to the possibility that FD 150kDa were cleared via the paracellular or endocytic mechanism present at the retina layer. In addition, the movements of microparticles were more restrictive and slower as compared to sodium fluorescein and FD 150kDa. This could be due to its hydrophobic interactions with collage fibers[7].

Moldow and coworkers[31] showed that the diffusion profile of fluorescein in the elderly liquefied vitreous was more homogeneous as opposed to a healthy vitreous. In addition, Foulds and colleagues demonstrated that hyaluronidase increased the clearance of tritiated water[9]. These studies demonstrated that small molecules were distributed and cleared faster in the liquefied vitreous system, an observation, which was also illustrated in our study on sodium fluorescein. Since diffusion is the main drive for the transport of small molecules, it is possible that diffusivity in liquefied vitreous may be enhanced.

On the other hand, the movement of large molecule depends on convective flow processes[23]. In partially liquefied vitreous, FD 150kDa was cleared faster which may indicate greater convective movement in the liquefied vitreous circulation. A lower concentration of FD 150kDa was detected in the liquefied vitreous, suggesting a faster rate of distribution and the capability of the vitreous in sustaining injected doses had significantly reduced. The plot derived from ocular fluorophotometry suggests that there was a temporary forward flux in partially liquefied vitreous model during the first few hours after injection. The same observation was not noted in a normal vitreous. This indicates that the flow processes in the liquefied vitreous generated this movement. Interestingly, forward flux was not evident in the case of sodium fluorescein. We may attribute this to the fact that sodium fluorescein diffused away faster than FD 150kDa, and thus if present, it may take place at the first few minutes after injection which was not captured in this study. The temporary forward flux of FD 150kDa in partially liquefied vitreous resulted in a steeper vitreous concentration gradient. However, the gradient pattern remained the same with the level of FD 150kDa reducing from anterior to posterior at later time points. Hence, we deduced that partial vitreous liquefaction increased the rate of material clearance but materials still moved along the same concentration gradient. More importantly, this observation could explain the need for more frequent injections of bevacizumab among the elderly population (mean age: 68.5 years; 3.75 injections) as compared to younger individuals (mean age: 39.5 years; 1.75 injections) seen clinically by Spielberg and Ley[32]. Therefore, for larger molecules such as antibodies and antibody fragments dosed into the vitreous, the faster rate of clearance in

partially liquefied vitreous has to be taken into consideration as part of current research investigating dosing schedule optimization in elderly patients.

In the case of 1 μm fluorescent particles, HRA was used to investigate the difference between the normal and liquefied vitreous models. The fluorescence signals from the microparticles measured with the ocular fluorophotometry had a high level of noise leading to unreliable data. HRA data shows that clusters of fluorescent microparticles were more scattered and sedimented faster under gravitational pull in the partially liquefied vitreous system versus the control eyes. Therefore, tissue exposure on the floor of the inferior quadrant of the eye may be greater in the more liquefied vitreous due to faster sedimentation of injected microparticles. In contrast, the local injection site will experience a higher concentration in a more gel-like vitreous, particularly if there is reflux back to the point of injection. Maurice proposed that particle sedimentation might increase the risk of dangerously high drug concentration achieved at the retina layer especially if the patient was sleeping in a supine position[33]. Localized multinuclear giant-cell reaction has also been reported around retina tissues that were in contact with the polymeric microspheres[34]. This information will be beneficial to the design of microparticulate formulations, in optimizing the particle size, drug loading, duration and rate of drug release as well as targeting to the desired site of action for the elderly population.

In summary, we have quantitatively established a reproducible partially liquefied vitreous model in laboratory rabbits that represented the degree of vitreous liquefaction occur in the general population of ages around 60 years. Therefore, it can serve as a useful investigative tool in the future of ocular

treatments for the elderly population. We have determined the percentage gel phase of unmodified rabbit vitreous and the result showed a close similarity to young human adults. Therefore, the use of juvenile animal models may underestimate the influence of convective forces present in the elderly patients, thereby overestimating drug efficacy. The joint operation of ocular fluorophotometry and HRA in current study provided a better understanding of intravitreal events. We managed to correlate data from both techniques in a quantitative manner. Unlike previous studies, we were able to relate the degree of vitreous liquefaction to material transport. Therefore, data provided in this study are more relevant to actual clinical situations. More studies are currently being undertaken in our laboratory to further understand the influence of vitreous liquefaction on drugs released from controlled release devices. However, the limitation of our current model is that it has neglected the influence of collagen fibers formed upon aging, which may be important for drug molecules prone to protein binding. Future studies should take this factor into consideration.

Acknowledgments

The authors are grateful to Professor Stephen Marshall and Paul Murray from the University of Strathclyde, Glasgow (Electronic and electrical engineering department) for their help in composing the Matlab program for HRA wide-angle image analysis. The detail of the program function will be described elsewhere.

References

1. Sebag J. Macromolecular Structure of the Corpus Vitreous. *Prog.Polym.Sci*. 1998; 23: 415-446.

2. Bishop PN. Structural Macromolecules and Supramolecular Organisation of the Vitreous Gel. *Prog Retin Eye Res.* 2000; 19(3): 323-344.

3. Balazs EA, Denlinger JL. *Aging changes in the vitreous. In Aging and Human Visual Function.* New York: Alan R. Liss; 1982: 45-47.

4. Sebag J. Balazs EA. Morphology and ultrastructure of human vitreous fibers. *Invest Ophthalmol Vis Sci.* 1989; 30 (8): 1867-1871.

5. Sebag J., Balazs EA. Human vitreous fibres and vitreoretinal disease. *Trans Ophthalmol Soc UK.* 1985; 104 (Pt 2): 123-8

6. Sebag J. Age-related changes in human vitreous structure. *Graefes Arch Clin Exp Ophthalmol.* 1987; 225: 89-93.

7. Peeters L, Sanders NN, Braeckmans K, et. al. Vitreous: A barrier to nonviral ocular gene therapy. *Invest Ophthalmol Vis Sci.* 2005; 46: 3553-3561.

8. Pitkänen L, Ruponen M, Nieminen J, et. al. Vitreous is a barrier in nonviral gene transfer by cationic lipids and polymers. *Pharm Res*. 2003; 20 (4): 576-583.

9. Foulds WS, Allan D, Moseley H, et. al. Effect of intravitreal hyaluronidase on the clearance of tritiated water from the vitreous to the choroid. *Br J Ophthalmol.*1985; 69: 529-532.

10. Sebag J, Ansari RR, Suh KI. Pharmacologic vitreolysis with microplasmin increases vitreous diffusion coefficients. *Graefes Arch Clin Exp Ophthalmol.* 2007; 245: 576-580.

11. Lee SS, Ghosn C, Yu Z, et. al. Vitreous VEGF clearance is increased following vitrectomy. *Invest Ophthalmol Vis Sci.* 2010; 51: 2135-2138.

12. Chin HS, Park TS, Moon YS, et. al. Difference in clearance of intravitreal triamcinolone acetonide between vitrectomized and nonvitrectomized eyes. *Retina*. 2005; 25(5): 556-560.

13. Ficker L, Meredith TA, Gardner S, et. al. Cefazolin levels after intravitreal injection. *Invest Ophthalmol Vis Sci*. 1990; 31 (3): 502-505.

14. Stepanova LV, Marchenko IY, Sychev GM. Direction of fluid transport in the lens. *Bull Exp Biol Med.* 2005; 139 (1): 50-51.

15. Harooni M, McMillan T, Refojo M. Efficacy and safety of enzymatic posterior vitreous detachment by intravitreal injection of hyaluronidase. *Retina*. 1998; 18:16-22.

16. Hikichi T, Kado M, Yoshida A. Intravitreal injection of hyaluronidase cannot induce posterior vitreous detachment in the rabbit. *Retina*. 2000; 20 (2): 195-198.

17. Wang ZL, Zhang X, Xu X, et. al. PVD following plasmin but not hyaluronidase: implications for combination pharmacologic vitreolysis therapy. *Retina*; 2005; 25: 38-43.

18. Tanaka M, Qui H. Pharmacological vitrectomy. *Seminars in Ophthalmology.* 2000; 15: 51-61.

19. Gottlieb JL, Antoszyk AN, Hatchell DL et. al. The safety of intravitreal hyaluronidase, a clinical and histologic study. *Invest Ophthalmol Vis Sci.* 1990; 31: 2345-2352.

20. Winkler BS, Cohn EM. Hyaluronidase and retinal function. *Arch Ophthalmol*. 1985; 103: 1743-1746.

21. Pirie A. The effect of hyaluronidase injection on the vitreous humor of the rabbit. *Br J Ophthalmol.* 1949; 33: 678-684.

22. Narayanan R, Kuppermann BD. Hyaluronidase for pharmacologic vitreolysis. *Dev Ophthalmol.* 2009; 44: 20-25.

23. Park J, Bungay PM, Lutz RJ, et.al. Evaluation of coupled convective-diffusive transport of drugs administered by intravitreal injection and controlled release implant. *J Control Release*. 2005; 105 (3): 279-295.

24. Worst JGF, Los LI. *Chapter 3: Functional anatomy of the vitreous. In Cisternal anatomy of the vitreous*. Amsterdam, Netherlands: Kugler Publications; 1995: pp. 33-48.

25. Stay MS, Xu J, Randolph TW, Barocas VH. Computer simulation of convective and diffusive transport of controlled-release drugs in the vitreous humor. *Pharm Res*. 2003; 20 (1): 96-102.

26. Xu J, Heys JJ, Barocas VH, et. al. Permeability and diffusion in vitreous humor: Implications for drug delivery. *Pharm Res*. 2000; 17(6): 664-669.

27. Araie M, Maurice DM. The loss of fluorescein, fluorescein glucuronide and fluorescein isothiocyanate dextran from the vitreous by the anterior and retinal pathways. *Exp Eye Res.* 1991; 52: 27-39.

28. Cunha-Vaz JG, Maurice DM. The active transport of fluorescein by the retinal vessels and the retina. *J. Physiol (Lond.)* 1967; 191: 467-486.

29. Takahashi J, Hikichi T, Mori F, et. al. Effect of nucleotide P2Y2 receptor agonists on outward active transport of fluorescein across normal blood-retina barrier in rabbit. *Exp Eye Res.* 2004; 78(1): 103-108.

30. Dias CS, Mitra AK. Vitreal elimination kinetics of large molecular weight FITC-labeled dextrans in albino rabbits using a novel microsampling technique. *J Pharm. Sci.* 2000; 89: 572-578.

31. Moldow B, Sander B, Larsen M, et.al. The effect of acetazolamide on passive and active transport of fluorescein across the blood-retina barrier in retinitis pigmentosa complicated by macular oedema. *Graefes Arch Clin Exp Ophthalmol*. 1998; 236: 881-889.

32. Spielberg L, Leys A. Intravitreal bevacizumab for hyopic choroidal neovascularization: short-term and 1-year results. Bull. Soc. Belge Ophtalmol. 2009; 312: 17-27.

33. Maurice D. Review: Practical issues in intravitreal drug delivery. *J Ocul Pharmacol Ther.* 2001; 17 (4): 393-401.

34. Giordano GG, Refojo MF, Arroyo MH. Sustained delivery of retinoic acid from microspheres of biodegradable polymer in PVR. *Invest Ophthalmol Vis Sci*. 1993; 34: 2743-2751.